Vol. 122: 43–55, 2016
doi: 10.3354/dao03062

DISEASES OF AQUATIC ORGANISMS
Dis Aquat Org

Published November 22

In situ hybridization and histopathological observations during ostreid herpesvirus-1-associated mortalities in Pacific oysters *Crassostrea gigas*

Rudolfo Bueno[1,*], Matthew Perrott[2], Magda Dunowska[2], Cara Brosnahan[1], Colin Johnston[1,3]

[1]Animal Health Laboratory, Investigation, Diagnostic Centres and Response—Wallaceville, Ministry for Primary Industries, 66 Ward St, PO Box 40742, Upper Hutt 5018, New Zealand

[2]Institute of Veterinary, Animal & Biomedical Sciences, Massey University Manawatu (Turitea) Tennent Drive, Palmerston North 4474, New Zealand

[3]*Present address:* Aquaculture New Zealand, Level 1 Wakatu House, Montgomery Square, Nelson 7010, New Zealand

ABSTRACT: In a previous longitudinal study conducted during a mortality investigation associated with ostreid herpesvirus-1 (OsHV-1) microvariant in New Zealand Pacific oysters in 2010–2011, temporality of OsHV-1 nucleic acid detection by real-time PCR assay and onset of Pacific oyster mortality was observed. The present study further elucidated the role of OsHV-1 using an *in situ* hybridization (ISH) assay on sections of Pacific oysters collected from the same longitudinal study. Hybridization of the labelled probe with the target region of the OsHV-1 genome in infected cells was detected colorimetrically using nitro blue tetrazolium (NBT). OsHV-1 presence and distribution in spat indicated by the ISH signal was then compared with the existence of pathological changes in oyster tissues. Dark blue to purplish black NBT cell labelling was seen predominantly in the stroma of the mantle and gills at Day 5 post introduction to the farm. The distribution and location of ISH signals indicated the extent of OsHV-1-infected cells in multiple tissues. Histopathological abnormalities were mostly non-specific; however, a progressive pattern of increasingly widespread haemocytosis coincided with the appearance of OsHV-1-infected cells in spat collected at different time-points. The visualisation of an increasing number of OsHV-1-positive cells in spat prior to a marked increase in mortality indicated the strong likelihood of an on-going and active viral infection in some oysters. Further studies are recommended to elucidate OsHV-1 pathogenesis in Pacific oysters in association with other potentially causal variables, such as elevated temperature and interaction with *Vibrio* spp. bacteria.

KEY WORDS: Ostreid herpesvirus-1 · Microvariant · µVar · Pacific oysters · *Crassostrea gigas* · *In situ* hybridization

INTRODUCTION

Oyster herpesviruses were recognised as important pathogens of bivalve molluscs in the early 1990s. The reference strain, ostreid herpesvirus 1 (OsHV-1) (GenBank AY509253), was established from a characterized herpesvirus isolate collected in 1995 from a Pacific oyster larva (Le Deuff & Renault 1999, Davison et al. 2005). OsHV-1 was then assigned to the *Malacoherpesviridae* family, order *Herpesvirales* (Davison et al. 2009).

Genomic variants, based mostly on polymorphism of the C2 and C6 region of the OsHV-1 genome, were reported, and they appeared to differ in virulence (Segarra et al. 2010, Martenot et al. 2012, Renault et al. 2012, Shimahara et al. 2012, Bai et al. 2015). Perio-

*Corresponding author: rudolfo.bueno@mpi.govt.nz

dic losses experienced by oyster-producing regions in the USA, France, Spain, Ireland, Mexico, New Zealand and Australia (Friedman et al. 2005, Vásquez-Yeomans et al. 2010, Roque et al. 2011, Jenkins et al. 2013, Keeling et al. 2014, Paul-Pont et al. 2014) have been attributed to several OsHV-1 variants. The existence of many OsHV-1 genotypic variants may also reflect the wide natural host range of bivalves susceptible to infection with the virus (Hine & Thorne 1997, Hine et al. 1998, Renault et al. 2000, 2001, Arzul et al. 2001a,b, Ren et al. 2013).

The occurrence of high mortalities in juvenile Pacific oysters *Crassostrea gigas* in New Zealand was investigated during the austral summer months of 2010–2011 (Bingham et al. 2013). The epidemic affected 73% of oyster growing areas in the north part of the North Island. Mortalities were estimated to range between 15 and 100% in spat and between 5 and 60% in adult oysters (Bingham et al. 2013). The ostreid herpesvirus detected from affected oysters was similar to the microvariant genotype previously reported from the northern hemisphere (Keeling et al. 2014). The OsHV-1 microvariant was detected from outbreaks of disease with unusually high mortalities in Pacific oyster spat and juveniles in France in 2008 (Segarra et al. 2010, Martenot et al. 2011). It is characterized by 12 successive nucleotide deletions between the C2 and C6 region of the virus genome when compared with the reference OsHV-1 strain (Martenot et al. 2011).

During the 2010–2011 outbreak, a short longitudinal study was conducted to investigate the temporal associations between development of the mortality syndrome and presence of selected pathogens. As a result, OsHV-1 microvariants were detected by real-time PCR in 83% of spat by Day 5 following transfer from hatchery to a farm experiencing high level (up to 100%) mortalities in the farmed oysters (Keeling et al. 2014). The aetiological role of OsHV-1 in the high losses experienced by the farm, while strongly suggested, was not fully established. This was partly due to lack of comparable data from unaffected farms during the longitudinal study, and partly due to the method of OsHV-1 detection employed. While real-time PCR provides a sensitive and specific assay for detection of viral nucleic acids, it does not differentiate between viruses accidently trapped in the gills or within the pallial cavity and those that established infection within the tissues. Since oysters are filter feeders, this distinction is important for inference of aetiological involvement. At the same time, the real-time PCR assay was not utilized to quantify viral loads and assess thresholds for differentiation between true infection and accidental presence of the virus in the tested samples (Oden et al. 2011, Paul-Pont et al. 2014). As such, the aims of the present study were to develop an *in situ* hybridization (ISH) assay for detection of OsHV-1 in oyster tissues and to use this assay to investigate the role of OsHV-1 in the oyster mortality event.

MATERIALS AND METHODS

Spat samples

Spat samples used in this study came from 2 sources. For the development of the OsHV-1 ISH assay, formalin-fixed paraffin-embedded (FFPE) tissues that had been previously confirmed to be either positive (n = 4) or negative (n = 3) for OsHV-1 DNA by real-time PCR were used. To further investigate the involvement of OsHV-1 in the 2010–2011 summer mortality event in New Zealand, 87 FFPE tissue samples from live spat collected during the previous study (Keeling et al. 2014) were examined (Table 1). The FFPE tissues, approximately 2–5 mm thick, were obtained from a transverse cut between the labial palps and adductor muscle of the spat and processed as described previously (Keeling et al. 2014).

In situ hybridization

The ISH procedure to detect target OsHV-1 nucleic acids in Pacific oysters was a modification from published protocols (Arzul et al. 2002, Barbosa-Solomieu et al. 2004, Meyer et al. 2005). The digoxigenin (DIG)-labelled, OsHV-1-specific DNA probe was prepared using a DIG PCR probe synthesis kit (Roche) using a plasmid containing OsHV-1 DNA as a template, according to the manufacturer's instructions. Briefly, approximately 700 bp PCR product amplified with primers C2 (5′-CTC TTT ACC ATG AAG ATA CCC ACC-3′) and C6 (5′-GTG CAC GGC TTA CCA TTT TT-3′) (Arzul et al. 2001b) was gel-purified and cloned into a plasmid vector pCR®4-TOPO® using TOPO TA Cloning Kit® for Sequencing (Invitrogen) with TOP10 chemically competent *E. coli*, according to the manufacturer's instructions. The efficiency of the DIG-labelling reaction was judged based on the comparison of sizes of the labelled product to the unlabelled control following agarose gel electrophoresis.

Oyster spat tissue sections (5 µm) on Superfrost-Plus® slides (Thermo Scientific) were dewaxed in

Table 1. Day of sampling (post introduction to the farm) for formalin fixed paraffin-embedded (FFPE) tissues used in the current study and the corresponding results after testing with *in situ* hybridization (ISH) and real-time PCR assay. For PCR, equivalent fresh mantle and gill tissue samples were tested in duplicate and considered positive for ostreid herpesvirus 1 (OsHV-1) if both replicates had a cut-off quantification cycle (Cq) value of ≤39, and negative if both or one replicate has a Cq value >39. Tissues were collected from Pacific oysters following introduction of healthy spat to the farm affected by high mortalities as described by Keeling et al. (2014). Dashes (–): no data (no sampling done or mortality not assessed)

Day of sampling	No. of FFPE tissues	ISH results (%)		Real-time PCR results (%)		% mortality
		No. positive	No. negative	No. positive	No. negative	
Day –1[a]	5	0	5 (100)	0	5 (100)	–
Day 1	7	0[b]	7 (100)	0	7 (100)	–
Day 3	7	0[b]	7 (100)	0	7 (100)	–
Day 5	17	8 (47.06)	9 (52.94)	14 (82.35)	3 (17.65)	–
Day 6	–	–	–	–	–	14
Day 7	17	10 (58.82)	7 (41.18)	17 (100.00)	0	–
Day 9	17	12 (70.59)	5 (29.41)	17 (100.00)	0	50
Day 13	17	2 (11.76)	15 (88.23)	14 (82.35)	3 (17.65)	70
Total	87	32 (36.78)	55 (63.22)	62 (71.26)	25 (28.73)	

[a]Pre-transfer. [b]ISH labelling was detected in the digestive lumen in one spat and not within the tissues. Thus, the spat was considered not infected with OsHV-1

xylene twice for 5 and 3 min, followed by rehydration in a series of graded ethanol solutions (100% ethanol 2 × 1 min; 96% ethanol 1 × 1 min; 80% ethanol 1 × 1 min; 50% ethanol 1 × 1 min). The slides were then rinsed with distilled water for 1 min and equilibrated with phosphate-buffered saline pH 7.4 (PBS) for 1 min. Protein digestion was performed using 100 µl of Proteinase K (100 µg ml^{-1}) in a humidified box at 37°C for 15 min. Protein hydrolysis was stopped by washing with 1.0% glycine in 1× PBS for 5 min. Tissue sections were then air dried briefly before the incubation with 100 µl of pre-hybridization buffer (50% formamide, 10% dextran sulphate, 4× saline sodium citrate [SSC] or SSC buffer, 250 µg ml^{-1} yeast tRNA, and 10% Denhardt solution) in a humid chamber at 42°C for 30 min. After the pre-hybridization step, coverslips were removed and excess liquid from around the edges blotted dry using lint-free tissue paper. A midsize Gene Frame® (ABgene Ltd) was mounted around the tissue, and the resultant trough was saturated with 60 µl of hybridization solution consisting of the pre-hybridization buffer with 2.3 ng $µl^{-1}$ of DIG-labelled DNA probe. The Gene Frame® was sealed with the coverslip, and the DNA on the slide was denatured at 95°C for 5 min using a flat solid metal platform placed inside the oven and cooled immediately for 5 min on ice. The slides were then moved to a humidified box and incubated overnight at the pre-determined hybridization temperature of 42°C. Post hybridization stringency washes were done in 2× SSC (5 min), followed by 1× SSC (5 min) at room temperature. The final wash was done using 0.75× SSC at 42°C (10 min).

After the final wash, tissue sections were equilibrated with 80–100 µl Solution I (100 mM maleic acid, 5 M NaCl, pH 7.5) for 5 min at room temperature, and they were incubated with blocking solution (DIG Nucleic Acid Detection Kit, Roche Diagnostics) for 30 min in a humidified chamber at room temperature. The hybridized probe was detected following incubation of sections with 80–100 µl of the anti-DIG alkaline phosphatase (AP) conjugate (diluted 1/500 in blocking solution) for 1 h at room temperature. Excess antibody was removed by 2 washes (1 min each) with Solution I and the slides then equilibrated with 100 µl Solution II (1 M Tris pH 8, 5 M NaCl, 1 M $MgCl_2$, pH 9) for 2 min at room temperature. To visualise DIG-labelled molecules, the slides were incubated with 80–100 µl of 5-bromo-4-chloro-3-indolyl phosphate with nitroblue tetrazolium salt (BCIP/NBT, Roche) diluted 1/50 in Solution II at room temperature for 1 h in the dark. Colour development was stopped by a brief rinse with distilled water and 1× PBS. The section was counter-stained with Bismarck Brown Y (Sigma-Aldrich) for 1 min and dehydrated in a series of ethanol washes of increasing concentration (96% ethanol 2 × 1 min; absolute ethanol 3 × 15 s). After clearing twice with xylene, tissue sections were mounted with a drop of Eukitt® resin (Fluka) and a cover slip. Once the mountant was dry, slides were examined using an Olympus BX51 microscope. Images were documented with a Colorview Soft Imaging camera in analySIS docu 5.0 software. Positive and negative controls were included in each run of the ISH and consisted of OsHV-1-positive and -negative tissue sections, as determined by prior

real-time PCR analysis. Non-specific binding of the probe was assessed by hybridisation of the OsHV-1-positive section with the control probe (hybridisation buffer without DIG-labelled probe). Non-specific staining due to the presence of endogenous alkaline phosphatase was assessed by omission of anti-DIG alkaline phosphatase conjugate during testing of the OsHV-1-positive sections. Tissue sections were considered positively labelled for OsHV-1 DNA if dark blue to black precipitates were visible within the cells and all controls showed expected results.

Evaluation of the archival oyster tissues

The distribution of OsHV-1 DNA in oyster tissues was assessed semi-quantitatively according to the intensity of staining and the number of OsHV-1-positive cells per organ. A grade of +, ++, and +++ was assigned for a low (1–5 positive cells), moderate (6–10 positive cells) or high (>10 positive cells) degree of ISH labelling. A total of 33 haematoxylin and eosin (H&E)-stained oyster tissues from the longitudinal study samples were also examined. The intensity, general distribution and specific location of the ISH signal determined which spat were evaluated for histopathological lesions and co-localisation with OsHV-1 DNA.

Comparison with real-time PCR

The results of the ISH assay were statistically compared with the results of a real-time PCR test conducted earlier using equivalent fresh mantle and gill tissues as described by Keeling et al. (2014). Relative agreement beyond chance between ISH and real-time PCR was analysed by a calculated kappa value. Initially, the frequency data (Table 2) from the 2 tests results were classified into a 4 cells of a 2×2 table (*a*: both test positive; *b*: real-time PCR negative and ISH positive; *c*: real-time PCR positive and ISH negative; and *d*: both test negative). The kappa value was calculated using the EpiTools developed by Ausvet Animal Health Services (http://epitools.ausvet.com.au/content.php?page=home) for diagnostic evaluation and comparison of 2 tests. The kappa value can range from −1 to +1. Agreement was evaluated with the following interpretation (Viera & Garrett 2005): kappa value of <0 is less than chance agreement, 0.01–0.20 has slight agreement, 0.21–0.40 has fair agreement, 0.41–0.60 is moderate agreement, 0.61–0.80 is substantial agreement and >0.8–1 is almost perfect agreement. Similarly, estimates of diagnostic sensitivity and specificity of ISH for the study population were described with real-time PCR as the reference method (Table 2). The OsHV-1 probe-based Taqman real-time PCR developed by the Animal Health Laboratory-Wallaceville, Ministry for Primary Industries, has a sensitivity of 95% and specificity of 99% (S. Keeling pers. comm. March 2011). The Epitools software was also used for this calculation (http://epitools.ausvet.com.au/content.php?page=Test Evaluation).

Table 2. Cross tabulation of *in situ* hybridization (ISH) and real-time PCR results to assess agreement using kappa value and to describe ISH test performance with real-time PCR as the reference method. Both kappa value and diagnostic test performance were calculated using EpiTools (http://epitools.ausvet.com.au/content.php?page=home). *a*: both test positive; *b*: real-time PCR negative and ISH positive; *c*: real-time PCR positive and ISH negative; *d*: both test negative. T+: test positive; T−: test negative

ISH	Real-time PCR		
	T+	T−	Total
T+	31 (*a*)	1 (*b*)	32
T−	31 (*c*)	24 (*d*)	55
Total	62	25	87

Kappa: 0.339 (CI 0.195–0.483). SE of kappa: 0.073
Sensitivity (Se) = $a/(a + c)$ = 0.50 (CI 0.370–0.630)
Specificity (Sp) = $d/(b + d)$ = 0.96 (CI 0.796–0.999)

RESULTS

ISH assay performance

OsHV-1-positive spat showed dark blue to purplish black-labelled cells as a consequence of the complementary hybridization of the C2C6 DIG-labelled probe with the viral genome. No labelling was detected in controls.

Detection of OsHV-1 DNA in archival oyster tissues

The distribution and sequential spread of OsHV-1 infection in oyster tissues and organs is shown in Fig. 1. OsHV-1 viral DNA was detected as dark blue to purplish black labelling in the nucleus and cytoplasm of cells (Fig. 2) located in the connective tissues of the mantle and gills as well as in the connective tissues beneath the primary digestive tract and secondary digestive ducts (Fig. 3). Labelled cells,

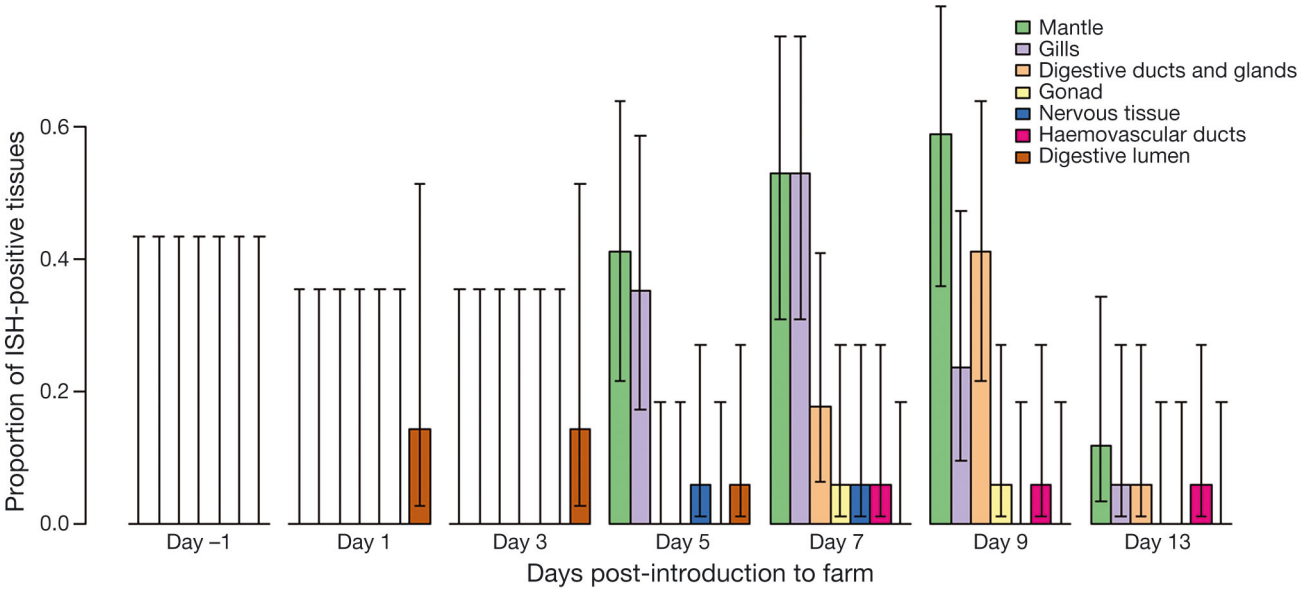

Fig. 1. Chronological appearance of ostreid herpesvirus 1 (OsHV-1)-specific hybridization signals in different tissues of Pacific oyster *Crassostrea gigas* spat before and after transfer to the OsHV-1-infected farm. Error bars are 95% CI

interpreted as circulating haemocytes, were also observed in various organs and tissues, including the gonads, nervous tissues and haemovascular ducts. Intensity of labelling signals in tissues was variable, but a consistent finding was the abundance of positive ISH signals in the connective tissue of the mantle. In addition, the nuclei of cells dispersed within the muscle fibres in the mantle tissue had a more intense hybridization signal (Fig. 2). These cells were also interpreted as OsHV-1-infected haemocytes.

Altogether, 32 of 87 (36.78%) oyster tissues were ISH positive for OsHV-1 DNA, and 55 of 87 (63.91%) were negative for OsHV-1 DNA by ISH (Table 1). No labelled cells were detected in spat collected a day prior to placement (Day –1). One spat sample collected at Day 1 post transfer and another at Day 3 post transfer showed ISH labelling in the digestive lumen but not within individual cells and were considered negative for OsHV-1 infection.

OsHV-1 infected cells were first detected at Day 5 post introduction to the infected farm. Out of 17 spat tested, 8 (47%) showed blue to purplish black labelling in various tissues. The incidence of ISH-positive oysters increased to 59% (10/17) at Day 7 and 71%

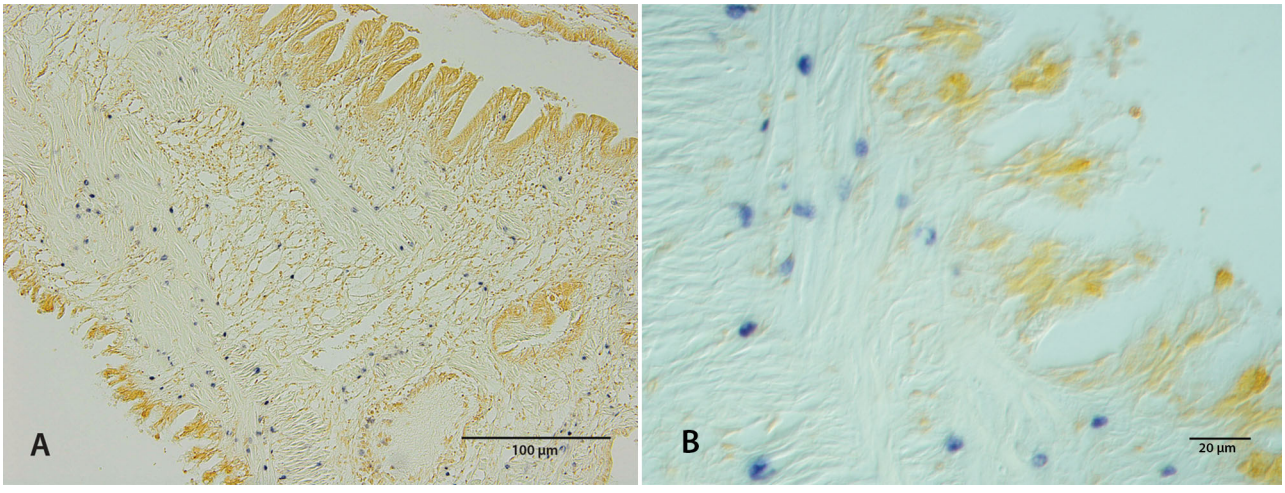

Fig. 2. (A) Dark blue hybridization labelling in cells of the stroma from a section of the mantle infected with ostreid herpesvirus-1 (OsHV-1). (B) Blue-labelled cells associated with the muscle fibres are most likely haemocytes. Differential phase contrast. Scale bars = (A) 100 µm, (B) 20 µm

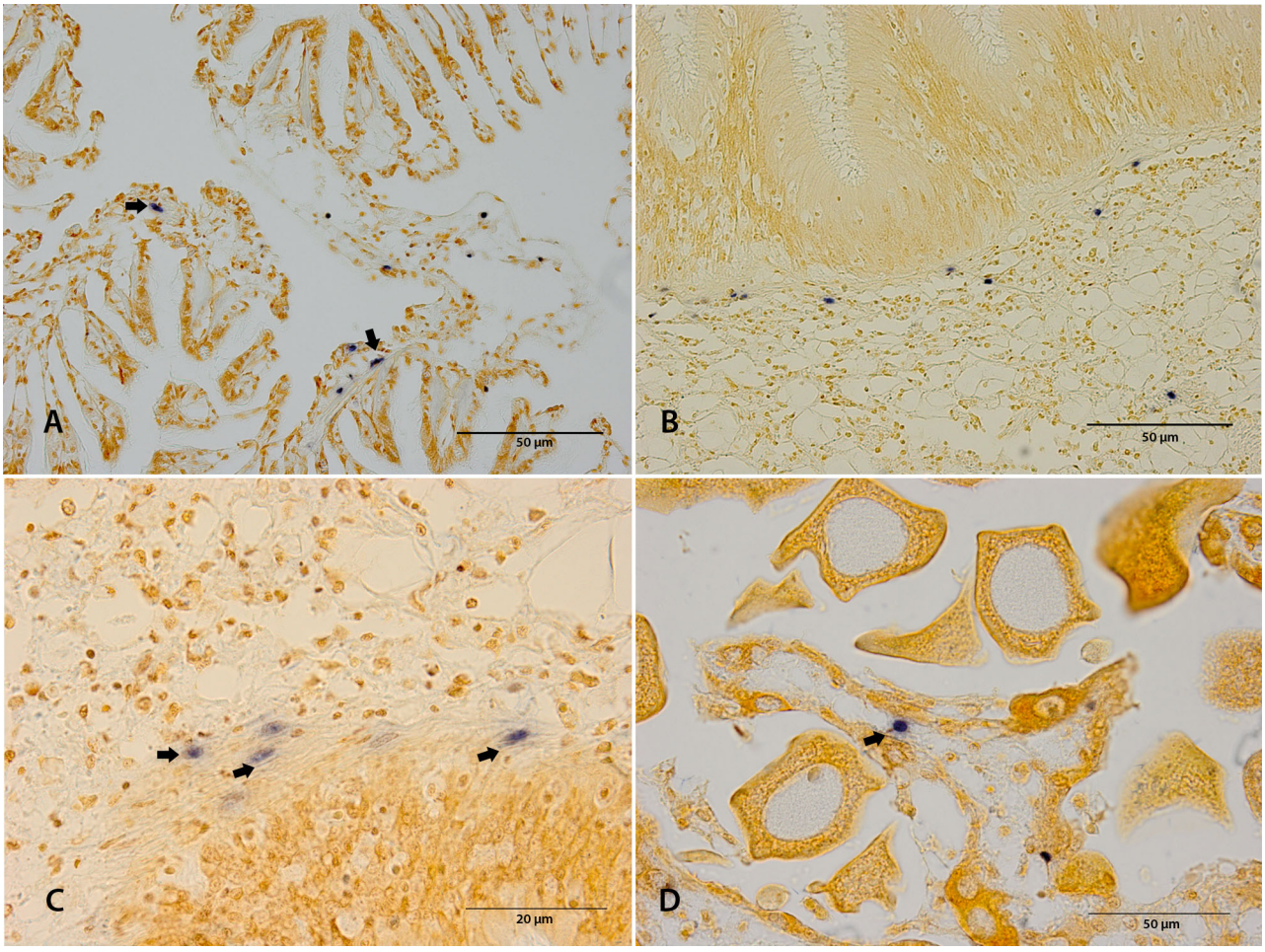

Fig. 3. Intense dark labelling (e.g. dark blue to purple-black-labelled cells with arrows) in (A) the connective tissue of the gills, (B,C) basal membrane of the digestive tract, and (D) in the lumen of gonad follicles interpreted as haemocytes. Scale bars = (A,B,D) 50 µm, (C) 20 µm

(12/17) at Day 9 post transfer. Only 2 out of 17 oysters (12%) were ISH positive at Day 13 post-placement. Based on the intensity of staining and the number of cells infected, severe infections (+++) were noted in spat collected from Days 5, 7 and 9. During these periods, ISH-labelled cells were predominantly confined to the mantle and gills, followed by occasional signals in the connective tissue surrounding the different parts of the digestive tract.

The proportion of oysters positive for OsHV-1 was higher when fresh tissues were tested by real-time PCR than when equivalent FFPE tissues were tested by ISH. The OsHV-1 prevalence by real-time PCR was 71.26% (62/87), with 28.73% (25/87) negative samples (Table 1). The total number of observed agreement between the 2 tests was 55 (63.22%), including 31 samples positive for OsHV-1 by both real-time PCR and ISH and 24 samples negative for OsHV-1 by both tests (Table 2). Most of the disagreements included samples that were positive for OsHV-1 by real-time PCR but negative by ISH (n = 31). One spat negative for OsHV-1 by real-time PCR, however, was positive by ISH. A fair agreement between the 2 tests, demonstrated by a kappa value of 0.339 (CI 0.195–0.483) was observed. The preliminary diagnostic sensitivity and specificity obtained for the ISH assay compared to real-time PCR as the reference test were 50 and 96.00% (Table 2), respectively.

Histopathological lesions and co-localization with OsHV-1 DNA

Although no pathognomonic pathological lesions were observed during the course of disease, several

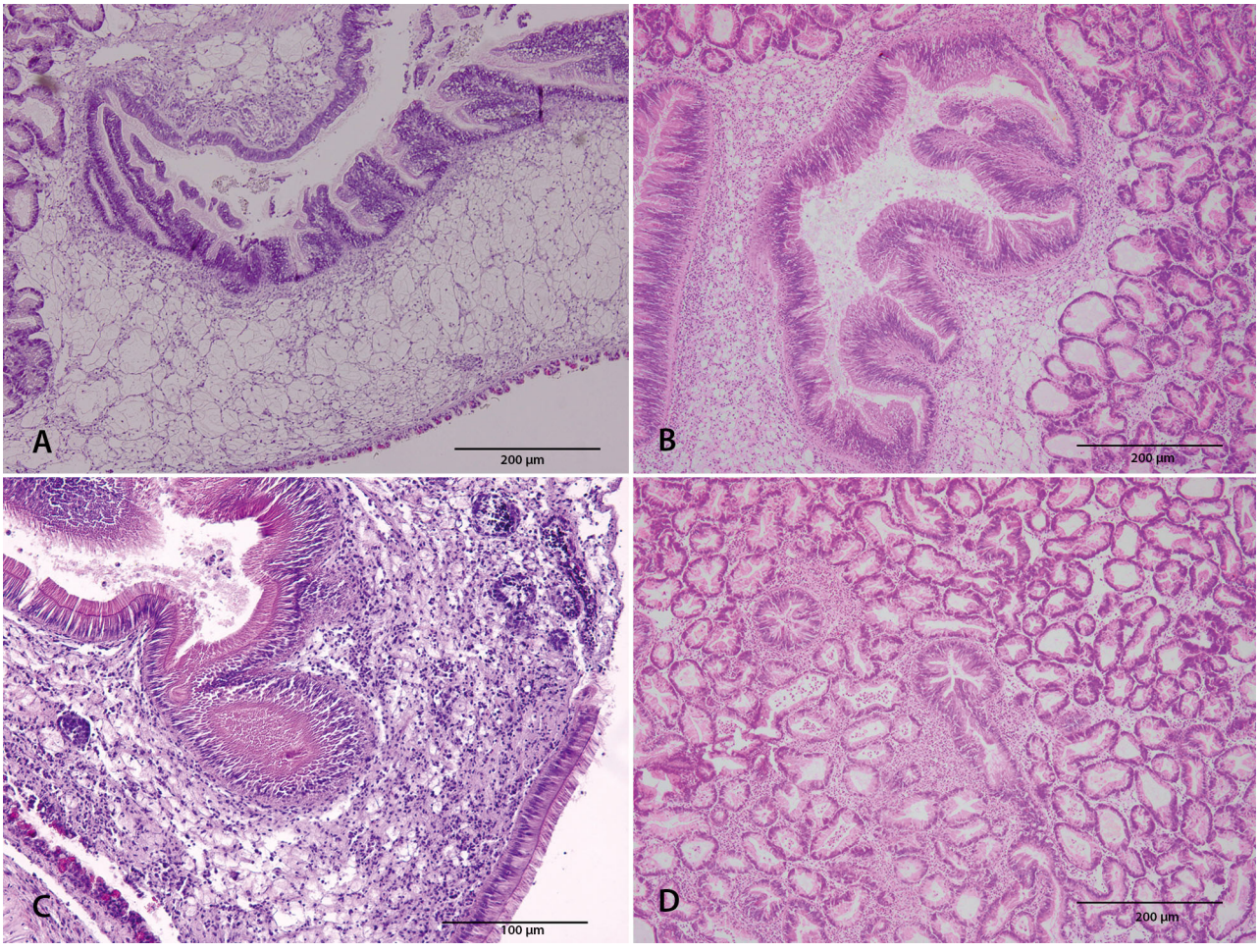

Fig. 4. Extent of haemocytosis in *Crassostrea gigas* spat varied from (A) mild and focal to (B) moderate and (C,D) extending to severe diffusion of cellular infiltrates. H&E stain. Scale bars = (A,B,D) 200 µm, (C) 100 µm

non-specific histological changes were observed in tissue sections from oysters during the study. One prominent example was the aggregation of haemocytes in tissues (haemocytosis) taken at Days 1 and 3 post transfer. This was also observed in spat sampled from the hatchery. Haemocytosis (Fig. 4) was observed either focally at discrete sites of inflammation or in the form of diffuse and systemic cellular infiltration in the stromal connective tissues. Haemocyte aggregations were particularly noticeable around major digestive ducts and tubules and in the stroma of the mantle sub-epithelium. Overall, it appeared that the degree and extent of haemocytosis transitioned from being focal, light to moderate haemocytosis (hatchery samples at Day −1, Day 1, and Day 3) to being diffuse and moderate to severe haemocytosis (Days 5, 7 and 9). In spite of these inflammatory cell-driven changes, there was no evidence for the presence of any intranuclear viral inclusions or other pathogenic agents detectable by light microscopy in the H&E-stained sections.

Degenerative lesions were also noted in the digestive glands in most tissue samples at all collection time-points but without an obvious pattern. These included different stages of epithelial atrophy of the diverticula, even within individual samples. In normal digestive diverticula, epithelial cells are tall and with either tri-radiate or quadri-radiate lumen. Some of the apparently abnormal tissues showed sloughed digestive gland epithelial cells in the lumen, and others had a dilated appearance due to reduction in height of the epithelium. Atrophy was seen predominantly in the peripheral region of the digestive glands although in some spat atrophy had a more general distribution.

Other non-specific changes that were occasionally seen included foci of necrosis evidenced by pyknosis and karyorrhexis in spat (Days 1 and 3) and diapedesis of haemocytes towards the digestive duct lumen

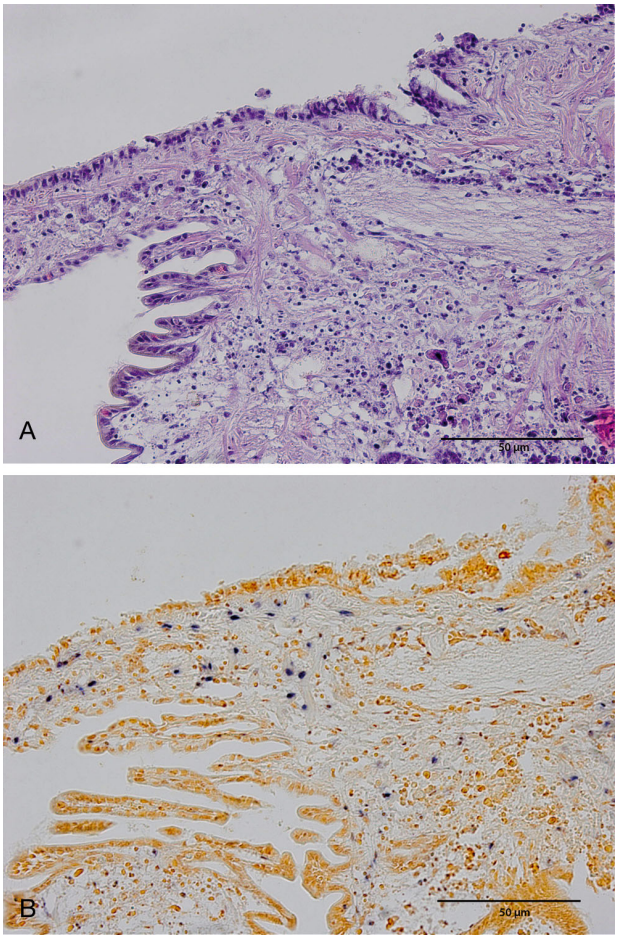

Fig. 5. (A) Cellular degeneration and necrosis in the mantle, co-localized with (B) a population of ostreid herpesvirus 1 (OsHV-1)-infected blue-labelled cells in the same consecutive section. H&E. Scale bars = 50 µm

(many different samples and time points). Focal and diffuse necrotic cell aggregates in mantle tissues and loss of tissue architecture of the gills and digestive ducts at Days 5 and 7 were also seen. Intra-nuclear inclusion bodies were not detected in any of the samples, but some chromatin margination in cells was seen in Day 7 samples. Another observation was an apparent increase in the number of multi-nucleated cells and brown-pigmented cells, so called, 'brown cells', in areas with necrosis.

Tissues taken at Days 5 and 7 post transfer revealed widespread cellular degeneration and necrotic foci in the connective tissues of the mantle and gills. In several instances, cellular changes were co-localised with the presence of OsHV-1-infected cells as determined by ISH. ISH signal in gills with extensive cellular necrosis detected in serially sectioned H&E-stained slides (Day 7) were observed. Necrotic cells (H&E stain) with pyknotic nuclei were also noted in the connective tissues of the mantle region within extensive distributions of OsHV-1 ISH-positive cells (Day 7) (Fig. 5). In a mantle section (Day 7) with haemocytic infiltration, the stromal tissue contained OsHV-1-infected cells distributed throughout the sub-epithelium and around the vascular ducts. In some slides, large cells that stained strongly with dark blue NBT labelling were seen within the muscle fibre bundles of the mantle pallial lobe and surrounded with aggregates of haemocytes.

DISCUSSION

This work was conducted to further our understanding on the role of OsHV-1 microvariant infection in Pacific oysters and its association with disease. To this end, development of an OsHV-1-specific ISH assay was undertaken. The presence of dark blue labelling within tissues positive for OsHV-1 by real-time PCR, together with absence of ISH signal in OsHV-1 PCR-negative tissues, probe controls and anti-DIG controls demonstrated that the assay was specific for detection of OsHV-1 DNA. The application of ISH for demonstrating viral infections has been described by others (Heino et al. 1989, Mabruk 2004, Deim et al. 2006). The test permits an investigator to determine which cells are susceptible to viral infection and characterize kinetics of the viral spread in tissues. This aspect of viral disease pathogenesis is very important, especially when studying emerging viruses (Chang et al. 1996).

Detection of OsHV-1 DNA in archival oyster tissues

In the current study, a hybridization signal for OsHV-1 in the gut lumen of one naïve spat (1/7), 1 d after exposure to an infected marine farm, indicated that one of the earliest entry points was via the digestive tract (Fig. 1). Evidence of OsHV-1 particles attached to particulates had been reported in water samples from areas with high mortalities in Pacific oysters (Paul-Pont et al. 2013, Evans et al. 2014). OsHV-1 particles in the intestine may have been ingested during filter feeding of the bivalve as soon as they were dispersed into the water column. The role of water as a medium for OsHV-1 transmission was previously elucidated in closed environment cohabitation trials (Schikorski et al. 2011) and in an open estuarine setting with high oyster mortalities (Paul-Pont et al. 2013, Evans et al. 2014). The low detection level of OsHV-1 at Day 1 was likely influ-

enced by different disease transmission mechanisms at play in the aquatic environment such as hydrodynamics, physical disturbances and density of infective virions in the water column (Paul-Pont et al. 2013).

Detectable individual cells containing OsHV-1 nucleic acids at Day 5 post transfer were found mostly in the connective tissue of the mantle and gills (Figs. 2 & 3). Infection of epithelial cells was not observed in this study. The positive ISH labelling thus implies that these organs (mantle and gills), with a transient population of haemocytes, were preferentially infected with the virus, and thus comprise suitable material for OsHV-1 diagnostic testing. Infected cell types observed in these tissues were small round cells most likely of the haemocyte class, fibroblast-like connective tissue cells, and cells associated with muscle fibres. The ISH signal in these tissues was particularly abundant and prominent in the cell nuclei. These observations are in agreement with the early reports (Arzul et al. 2002, Lipart & Renault 2002) wherein connective tissues of *C. gigas* spat and adults were the main target of OsHV-1 infection. Interestingly, the identity of infected cells with large nuclei associated with muscle bundles in the mantle was difficult to establish. Initially, labelled cells were thought to be myocytes, but eventually we interpreted them as more likely to be haemocytes. Others (Lipart & Renault 2002, Corbeil et al. 2015) also detected OsHV-1 DNA by ISH in muscle cells in the mantle, as well as in adductor muscle and cells in the heart ventricle.

Some infected cells were also present within the periphery of nervous tissue but were not as abundant as ISH-positive cells in the mantle and gills. Although sites of latency for OsHV-1 are not currently known (Davison et al. 2005, Segarra et al. 2014), it is possible that, similar to other alphaherpesviruses, OsHV-1 establishes latency in the nerve tissue. Alphaherpesviruses that infect vertebrate animals have a predilection for establishing active infection in epithelial cells and establishing latency in neuronal cells (Krummenacher et al. 2013). Persistence of OsHV-1 in adult Pacific oysters without associated clinical signs and mortalities has been previously reported (Arzul et al. 2002), and the nerve tissue was a suggested site for latency (Lipart & Renault 2002). In this work, however, ISH-positive cells in the nerve tissue were more likely haemocytes that were associated with the haemolymph supply. Haemocyte infiltrations were also observed in the nerve tissues of the gastropod abalone infected with another mollusc virus, the abalone herpesvirus (Hooper et al. 2007).

Occasional labelling of cells was also observed around and within the male and female gonads, including the germinal reproductive areas, but the significance of these findings remains unclear. Vertical transmission of OsHV-1 from asymptomatic parent stock was considered when a herpesvirus-like infection was detected in early larval stages (Le Deuff et al. 1996, Barbosa-Solomieu et al. 2005). This hypothesis was further reinforced by ISH and immunohistochemistry (IHC) detection of viral DNA and proteins in the connective tissues of male and female gonads, including female egg cells of adult Pacific oysters (Arzul et al. 2002). The infected gametes could contaminate developing embryos during discharge and spawning.

ISH and real-time PCR comparison

The results of OsHV-1 ISH were in fair agreement (kappa = 0.339) (95% CI = 0.195–0.483) with results of real-time PCR testing (Table 2). Fair implies a reasonable level of disparity, which may be explained in more than one way. Firstly, the type of material used for testing differed between the 2 tests. Fresh tissues were used for real-time PCR, whereas FFPE tissues were used for ISH. Formalin fixation degrades nucleic acids in tissues. At the same time, the cross linking of proteins around the remaining segments of nucleic acids may render them unavailable for detection (Bancroft & Gamble 2008). In addition to incomplete target sequences, failure to optimally expose DNA during tissue pre-treatment processes such as Proteinase K digestion reduces the sensitivity of the technique (Lu et al. 1995). Finally, PCR techniques involve exponential amplification of low copy numbers to a point where detection is possible, whereas ISH allows for only modest and linear signal amplification based on the number of DIG labels per strand and the constraints imposed by antibody–enzyme binding and chromogen build up. It should be noted, however, that positive results in real-time PCR, particularly those with high quantification cycle (Cq) values must be interpreted with caution when ascertaining true OsHV-1 infection in oyster. It is always possible that false positive results may arise in real-time PCR due to amplification of viral nucleic acids present in the water environment surrounding the oyster, outside the mantle and gills or within the gut lumen. Despite the fact that this OsHV-1 ISH assay had low diagnostic sensitivity and high specificity relative to our reference real-time PCR assay (Table 2), due to the ability to visualise OsHV-1-

infected cells, it may be a test of choice for selected purposes, such as confirming an OsHV-1 infection in an outbreak situation.

Histopathological lesions and co-localization with OsHV-1 DNA

In general, non-specific histological changes were detected in all tissues examined. A pattern of progressive pathological anomaly commonly observed in disease processes of vertebrate animals was not evident. However, tissue changes such as aggregation of haemocyte cells, epithelial thinning or atrophy of the digestive gland and foci of tissue lysis are largely viewed as physiological, perhaps immunological, coping mechanisms of bivalve molluscs against environmental stresses, infection with primary pathogenic agents or concurrent secondary infections (Sparks 1972). Thus, such findings in this study, although seemingly unclear, may have been important pieces in the broader pathogenesis of OsHV-1 infection if the story could be told through a greater number of sampling time points.

Haemocytosis, or the infiltrations of haemocytes in all organs, although common across the different sampling time-points (Fig. 4), appeared to be more severe in spat collected at Day 5 and onwards. In bivalve molluscs, the aggregation of haemocytes represents a host cellular response with an aim to destroy, dilute and isolate unwanted agents (Sparks & Morado 1988). This cell type is also responsible for clearing dead cells and tissue debris. Hence, the increase in the proportion of spat with widespread haemocytosis is probably due to a marked inflammatory reaction to virus-infected cells or the presence of necrotic tissue (Sparks & Morado 1988). This finding of haemocytosis is consistent with various reports of OsHV-1 infections (Burge et al. 2006, Jenkins et al. 2013). Widespread haemocytic infiltration surrounding ulcerated labial palps and necrotic gills was also seen in Portuguese oyster infected with gill necrosis virus (GNV) and in *Crassostrea angulata* infected with haemocytic infection viruses (HIV) (Comps 1988).

Interpretation of this immunological event was complicated by the culture of *Vibrio* spp. bacteria in the study cohort as shown in a separate report (Keeling et al. 2014). *V. alginolyticus* was detected in spat from the hatchery followed by identification of several other *Vibrio* species (*V. splendidus*, *V. chagassi*, *V. aestuarianus*) on subsequent sampling days by sequencing of the *atpA* gene from these bacterial cultures. Although the presence of these bacteria may have contributed to the observed histological alterations, haemocyte infiltration around bacterial foci, as described by Elston et al. (1987), was not evident.

Digestive gland atrophy was variable in almost all samples, although areas of thinner digestive tubule epithelium were observed predominantly in samples from Day 9 post transfer. Atrophy of the digestive gland is attributed to various factors and considered to be a good indicator of unfavourable environmental conditions (Sparks 1972). Low oxygen tension during high summer temperatures (Fogelson et al. 2011), spawning stress (Kang et al. 2010), salinity changes (Knowles et al. 2014), toxin-producing dinoflagellates (Pearce et al. 2005) and starvation (Winstead 1995) have all been shown to induce sloughing of gut cells resulting in thin, dilated digestive glands in oyster bivalves. Thinning of the digestive diverticulae was also reported to be an early feature, within 8 h, of acute inflammation in *C. gigas* (Sparks & Morado 1988).

Areas of tissue necrosis were observed on Days 5, 7 and 9 post transfer and usually involved the mantle, gills and alimentary tract. Mantle and gills were the most affected organs in terms of both the numbers of infected cells and the intensity of the positive signals. An interesting finding here was the presence of ISH signal in areas with haemocyte aggregations and cell necrosis (Fig. 5). Although the significance of this discovery is difficult to ascertain, it indicates that haemocyte infiltrations may have occurred as a response to the presence of virus-infected cells or necrotic debris from cell destruction in the wake of viral replication. Notably, spat samples from Day 9 appeared to be intact and morphologically normal compared to spat from Days 5 and 7. It is presumed that in this single time cohort, a group of resistant oysters started to emerge as the highly susceptible spat declined in numbers due to mortalities. Certain individuals or age classes of oysters are more likely to survive infection, continue to produce virus particles or act as asymptomatic carriers (Degremont & Benabdelmouna 2014).

Another finding was the prominent appearance of 2 types of cells, multi-nucleated cells and large cells with brown-pigmented cytoplasm, at Day 9 post-transfer. These cell types are believed to participate in clearing cellular debris (Sparks & Morado 1988). Brown cell numbers were observed to increase during inflammation, which suggest that they may participate in tissue defence (Zaroogian & Yevich 1994). According to a study by Zaroogian & Yevich (1994) in *C. virginica*, brown cells contain lysosomes, which help in the detoxification and degradation of internalised soluble foreign debris from the hemolymph.

The appearance of these cells at a relatively late stage of the sampling regime in this study suggests that some oysters may have survived long enough to develop an innate cellular immune and stress response (Takahashi & Muroga 2008).

CONCLUSIONS

Establishing causation in any disease outbreak is important in order to develop an effective intervention strategy. The elucidation of cause and effect, however, is not a straightforward process and requires compelling arguments derived from observational events and experimental evidence to prove causal linkage. OsHV-1 infection was concluded to be a necessary cause, in addition to other multiple risk factors including elevated temperature, for the summer mortalities among the farmed Pacific oysters in New Zealand in 2010–2011 (Bingham et al. 2013). This inference was attributed to consistent detection of the virus nucleic acid in oysters from all affected farms, the detection of OsHV-1 during the short longitudinal study conducted and the similarity of the virus detected from the outbreak to the sequenced microvariant that caused widespread mortality of *Crassostrea gigas* in France in 2008. Using the ISH technique, we have further strengthened these conclusions by demonstrating that Pacific oysters were in fact infected with OsHV-1. Whilst the positive ISH result does not necessarily indicate viral replication, the visualisation of an increasing number of OsHV-1-infected cells in spat prior to marked increase in mortality described by Keeling et al. (2014) indicated an on-going active infection. Such a temporal relationship is an important criterion to build the case and to corroborate the causal link between OsHV-1 infection and spat mortalities. The influence of other pathogens such as *Vibrio* spp., in conjunction with increased water temperatures for occurrence of high mortalities in Pacific oyster spat, however, needs to be further elucidated.

Acknowledgements. We express our appreciation to Dr. Brian Jones and Dr. Richard Spence for the critical review of the paper. Special thanks also to the Animal Health Laboratory, Investigation and Diagnostic Centre and Response, Ministry for Primary Industries (MPI) at Wallaceville and Institute of Veterinary, Animal & Biomedical Sciences (IVABS), Massey University, for funding and supporting the conduct of this investigation. We also acknowledge Dr. Suzanne Keeling for sharing her molecular expertise during the Pacific oyster mortality investigation of 2010–2011 and Dr. Stuart Hunter for helping interpret the histopathology slides.

LITERATURE CITED

Arzul I, Nicolas JL, Davison AJ, Renault T (2001a) French scallops: a new host for ostreid herpesvirus-1. Virology 290:342–349

Arzul I, Renault T, Lipart C, Davison AJ (2001b) Evidence for interspecies transmission of oyster herpesvirus in marine bivalves. J Gen Virol 82:865–870

Arzul I, Renault T, Thébault A, Gérard A (2002) Detection of oyster herpesvirus DNA and proteins in asymptomatic *Crassostrea gigas* adults. Virus Res 84:151–160

Bai C, Wang C, Xia J, Sun H, Zhang S, Huang J (2015) Emerging and endemic types of *Ostreid herpesvirus 1* were detected in bivalves in China. J Invertebr Pathol 124:98–106

Bancroft JD, Gamble M (2008) Theory and practice of histological techniques. Churchill Livingstone, Edinburgh

Barbosa-Solomieu V, Miossec L, Vázquez-Juárez R, Ascencio-Valle F, Renault T (2004) Diagnosis of ostreid herpesvirus 1 in fixed paraffin-embedded archival samples using PCR and *in situ* hybridisation. J Virol Methods 119: 65–72

Barbosa-Solomieu V, Dégremont L, Vázquez-Juárez R, Ascencio-Valle F, Boudry P, Renault T (2005) Ostreid herpesvirus 1 (OsHV-1) detection among three successive generations of Pacific oysters (*Crassostrea gigas*). Virus Res 107:47–56

Bingham P, Brangenberg N, Williams R, Van Andel M (2013) Investigation into the first diagnosis of ostreid herpesvirus type 1 in Pacific oysters. Surveillance 40:20–24

Burge CA, Griffin FJ, Friedman CS (2006) Mortality and herpesvirus infections of the Pacific oyster *Crassostrea gigas* in Tomales Bay, California, USA. Dis Aquat Org 72: 31–43

Chang PS, Lo CF, Wang YC, Kou GH (1996) Identification of white spot syndrome associated baculovirus (WSBV) target organs in the shrimp *Penaeus monodon* by *in situ* hybridisation. Dis Aquat Org 27:131–139

Comps M (1988) Epizootic diseases of oysters associated with viral infections. Am Fish Soc Spec Publ 18:23–37

Corbeil S, Faury N, Segarra A, Renault T (2015) Development of an *in situ* hybridization assay for the detection of ostreid herpesvirus type 1 mRNAs in the Pacific oyster, *Crassostrea gigas*. J Virol Methods 211:43–50

Davison AJ, Trus BL, Cheng N, Steven AC and others (2005) A novel class of herpesvirus with bivalve hosts. J Gen Virol 86:41–53

Davison AJ, Eberle R, Ehlers B, Hayward GS and others (2009) The order *Herpesvirales*. Arch Virol 154:171–177

Degremont L, Benabdelmouna A (2014) Mortality associated with OsHV-1 in spat *Crassostrea gigas*: role of wild-caught spat in the horizontal transmission of the disease. Aquacult Int 22:1767–1781

Deim Z, Szeredi L, Tompó V, Egyed L (2006) Detection of bovine herpesvirus 4 in aborted bovine placentas. Microb Pathog 41:144–148

Elston R, Beattie J, Friedman C, Hedrick R, Kent M (1987) Pathology and significance of fatal inflammatory bacteraemia in the Pacific oyster, *Crassostrea gigas* Thünberg. J Fish Dis 10:121–132

Evans O, Paul-Pont I, Hick P, Whittington R (2014) A simple centrifugation method for improving the detection of ostreid herpesvirus-1 (OsHV-1) in natural seawater samples with an assessment of the potential for particulate attachment. J Virol Methods 210:59–66

Fogelson SB, Rikard FS, Brady Y, Wallace RK (2011) Histopathology of the digestive tissues and whole-body anaerobic bacteria counts of the Eastern oyster, *Crassostrea virginica*, after experimental exposure to anoxia. J Shellfish Res 30:627–634

Friedman CS, Estes RM, Stokes NA, Burge CA and others (2005) Herpes virus in juvenile Pacific oysters *Crassostrea gigas* from Tomales Bay, California, coincides with summer mortality episodes. Dis Aquat Org 63:33–41

Heino P, Hukkanen V, Arstila P (1989) Detection of human papilloma virus (HPV) DNA in genital biopsy specimens by *in situ* hybridization with digoxigenin-labeled probes. J Virol Methods 26:331–337

Hine PM, Thorne T (1997) Replication of herpes-like viruses in haemocytes of adult flat oysters *Ostrea angasi*: an ultrastructural study. Dis Aquat Org 29:189–196

Hine PM, Wesney B, Besant P (1998) Replication of a herpes-like virus in larvae of the flat oyster *Tiostrea chilensis* at ambient temperatures. Dis Aquat Org 32:161–171

Hooper C, Hardy-Smith P, Handlinger J (2007) Ganglioneuritis causing high mortalities in farmed Australian abalone (*Haliotis laevigata* and *Haliotis rubra*). Aust Vet J 85:188–193

Jenkins C, Hick P, Gabor M, Spiers Z and others (2013) Identification and characterisation of an ostreid herpesvirus-1 microvariant (OsHV-1 µ-var) in *Crassostrea gigas* (Pacific oysters) in Australia. Dis Aquat Org 105: 109–126

Kang DH, Chu FLE, Yang HS, Lee CH, Koh HB, Choi KS (2010) Growth, reproductive condition, and digestive tubule atrophy of Pacific oyster *Crassostrea gigas* in Gamakman Bay off the southern coast of Korea. J Shellfish Res 29:839–845

Keeling SE, Brosnahan CL, Williams R, Gias E and others (2014) New Zealand juvenile oyster mortality associated with ostreid herpesvirus 1 — an opportunistic longitudinal study. Dis Aquat Org 109:231–239

Knowles G, Handlinger J, Jones B, Moltschaniwskyj N (2014) Hemolymph chemistry and histopathological changes in Pacific oysters (*Crassostrea gigas*) in response to low salinity stress. J Invertebr Pathol 121:78–84

Krummenacher C, Carfí A, Eisenberg RJ, Cohen GH (2013) Entry of herpesviruses into cells: the enigma variations. In: Pöhlmann S, Simmons G (eds) Viral entry into host cells. Springer, New York, NY, p 178–195

Le Deuff RM, Renault T (1999) Purification and partial genome characterization of a herpes-like virus infecting the Japanese oyster, *Crassostrea gigas.* J Gen Virol 80: 1317–1322

Le Deuff RM, Renault T, Gérard A (1996) Effects of temperature on herpes-like virus detection among hatchery-reared larval Pacific oyster *Crassostrea gigas.* Dis Aquat Org 24:149–157

Lipart C, Renault T (2002) Herpes-like virus detection in infected *Crassostrea gigas* spat using DIG-labelled probes. J Virol Methods 101:1–10

Lu QL, Lawson P, Thomas JA (1995) Criteria for consistent and high sensitivity of DNA *in situ* hybridization on paraffin sections: optimal proteolytic enzyme digestion. J Clin Lab Anal 9:285–292

Mabruk MJEMF (2004) *In situ* hybridization: detecting viral nucleic acid in formalin-fixed, paraffin-embedded tissue samples. Expert Rev Mol Diagn 4:653–661

Martenot C, Oden E, Travaillé E, Malas JP, Houssin M (2011) Detection of different variants of Ostreid Herpesvirus 1 in the Pacific oyster, *Crassostrea gigas* between 2008 and 2010. Virus Res 160:25–31

Martenot C, Fourour S, Oden E, Jouaux A, Travaillé E, Malas JP, Houssin M (2012) Detection of the OsHV-1 µVar in the Pacific oyster *Crassostrea gigas* before 2008 in France and description of two new microvariants of the ostreid herpesvirus 1 (OsHV-1). Aquaculture 338–341: 293–296

Meyer GR, Bower SM, Carnegie RB (2005) Sensitivity of a digoxigenin-labelled DNA probe in detecting *Mikrocytos mackini*, causative agent of Denman Island disease (mikrocytosis), in oysters. J Invertebr Pathol 88:89–94

Oden E, Martenot C, Berthaux M, Travaillé E, Malas JP, Houssin M (2011) Quantification of ostreid herpesvirus 1 (OsHV-1) in *Crassostrea gigas* by real-time PCR: determination of a viral load threshold to prevent summer mortalities. Aquaculture 317:27–31

Paul-Pont I, Dhand NK, Whittington RJ (2013) Spatial distribution of mortality in Pacific oysters *Crassostrea gigas*: reflection on mechanisms of OsHV-1 transmission. Dis Aquat Org 105:127–138

Paul-Pont I, Evans O, Dhand NK, Rubio A, Coad P, Whittington R (2014) Descriptive epidemiology of mass mortality due to *Ostreid herpesvirus-1* (OsHV-1) in commercially farmed Pacific oysters (*Crassostrea gigas*) in the Hawkesbury River estuary. Aust Aquacult 422–423:146–159

Pearce I, Handlinger JH, Hallegraeff GM (2005) Histopathology in Pacific oyster (*Crassostrea gigas*) spat caused by the dinoflagellate *Prorocentrum rhathymum.* Harmful Algae 4:61–74

Ren W, Chen H, Renault T, Cai Y, Bai C, Wang C, Huang J (2013) Complete genome sequence of acute viral necrosis virus associated with massive mortality outbreaks in the Chinese scallop, *Chlamys farreri*. Virol J 10:110

Renault T, Le Deuff RM, Chollet B, Cochennec N, Gérard A (2000) Concomitant herpes-like virus infections in hatchery-reared larvae and nursery-cultured spat *Crassostrea gigas* and *Ostrea edulis.* Dis Aquat Org 42: 173–183

Renault T, Lipart C, Arzul I (2001) A herpes-like virus infects a non-ostreid bivalve species: virus replication in *Ruditapes philippinarum* larvae. Dis Aquat Org 45:1–7

Renault T, Moreau P, Faury N, Pepin JF, Segarra A, Webb SC (2012) Analysis of clinical ostreid herpesvirus 1 (*Malacoherpesviridae*) specimens by sequencing amplified fragments from three virus genome areas. J Virol 86: 5942–5947

Roque A, Carrasco N, Andree KB, Lacuesta B and others (2011) First report of OsHV-1 microvar in Pacific oyster (*Crassostrea gigas*) cultured in Spain. Aquaculture 324: 303–306

Schikorski D, Faury N, Pepin JF, Saulnier D, Tourbiez D, Renault T (2011) Experimental ostreid herpesvirus 1 infection of the Pacific oyster *Crassostrea gigas*: kinetics of virus DNA detection by q-PCR in seawater and in oyster samples. Virus Res 155:28–34

Segarra A, Pépin JF, Arzul I, Morga B, Faury N, Renault T (2010) Detection and description of a particular *Ostreid herpesvirus 1* genotype associated with massive mortality outbreaks of Pacific oysters, *Crassostrea gigas*, in France in 2008. Virus Res 153:92–99

Segarra A, Baillon L, Tourbiez D, Benabdelmouna A, Faury N, Bourgougnon N, Renault T (2014) Ostreid herpesvirus type 1 replication and host response in adult Pacific oysters, *Crassostrea gigas.* Vet Res 45:103

Shimahara Y, Kurita J, Kiryu I, Nishioka T and others (2012) Surveillance of type 1 ostreid herpesvirus (OsHV-1) variants in Japan. Fish Pathol 47:129–136

Sparks A (1972) Invertebrate pathology noncommunicable diseases. Academic Press, New York, NY

Sparks AK, Morado JF (1988) Inflammation and wound repair in bivalve molluscs. Am Fish Soc Spec Publ 18: 139–152

Takahashi KG, Muroga K (2008) Cellular defense mechanisms in bivalve molluscs. Fish Pathol 43:1–17

Vásquez-Yeomans R, García-Ortega M, Cáceres-Martínez J (2010) Gill erosion and herpesvirus in *Crassostrea gigas* cultured in Baja California, Mexico. Dis Aquat Org 89: 137–144

Viera AJ, Garrett JM (2005) Understanding interobserver agreement: the kappa statistic. Fam Med 37:360–363

Winstead JT (1995) Digestive tubule atrophy in eastern oysters, *Crassotrea virginica* (Gmelin, 1791), exposed to salinity and starvation stress. J Shellfish Res 14:105–112

Zaroogian G, Yevich P (1994) The nature and function of the brown cell in *Crassostrea virginica*. Mar Environ Res 37: 355–373

Editorial responsibility: Stephen Feist, Weymouth, UK

Submitted: June 6, 2016; Accepted: September 12, 2016
Proofs received from author(s): November 16, 2016